EFFECT OF BURIED PHONONIC CRYSTAL BARRIERS IN STRATIFIED MEDIUM

PACS: 43.40.Tm

Albino, Carlos[1]; Godinho, Luís[1]; Alves Costa, Pedro[2]; Amado Mendes, Paulo[1]

[1]ISISE, Departamento de Engenharia Civil, Universidade de Coimbra, Rua Luís Reis Santos - Pólo II da Universidade, 3030-788 Coimbra, Portugal
{capa@uc.pt, lgodinho@dec.uc.pt, pamendes@dec.uc.pt }

[2]Construct-FEUP, University of Porto, Rua Dr. Roberto Frias, 4200-465 Porto, Portugal
{pacosta@fe.up.pt}

Keywords: Numerical modelling, Phononic crystals, Vibration mitigation

ABSTRACT

Vibration induced by vehicles is a significant problem in large cities causing a major impact on human activities, comfort and health. Innovative protection strategies based on “phononic” crystals have recently been developed. Previous research already demonstrated the possibility to filter the most dominant vibration frequencies. The work presented in this paper is an extension of previously developed work in order to study the influence of a hypothetical layered structure of the propagation medium. This work uses a 3D FEM model to perform several simulations, which are implemented with a very efficient time-marching algorithm, as has been shown in previous works.

RESUMO

A vibração induzida por veículos é um problema significativo nas grandes cidades, causando um grande impacto nas atividades humanas, conforto e saúde. Estratégias inovadoras de proteção baseadas em cristais fónicos foram desenvolvidas recentemente. Pesquisas anteriores já demonstraram a possibilidade de filtrar as frequências de vibração mais dominantes. O trabalho apresentado neste artigo é uma extensão de trabalhos prévios no sentido de estudar a influência de uma hipotética constituição em camadas do meio de propagação. Este trabalho recorre a um modelo FEM 3D para realizar várias simulações que são implementadas com um algoritmo de marcha no tempo muito eficiente, como foi demonstrado em trabalhos anteriores.

INTRODUCTION

Wave propagation is currently a topic of extreme importance in Civil Engineering. A current concern of civil engineers is related to the mitigation of vibrations triggered by the heavy transport traffic, both by road and rail, which causes mechanical waves that propagate through the ground and can directly interfere with sensible buildings and human comfort and well-being. This is a topic that has been under discussion since the middle of last century when high-speed trains, with speeds above 200 km/h, emerged as regular intercity transport [1–3]. Currently, an increase in the capacity of the rail network is expected throughout Europe. This increase should receive special attention in urban areas where efficient solutions for the mitigation of vibrations induced by the passage of trains should be implemented in order to achieve widespread social acceptance. The classical strategies to mitigate this type of vibrations are the well-known trenches, buried walls and blocks of inertia. Recently, researchers have developed new and innovative methods based on a physical concept already widely known in the acoustics world, more specifically in the acoustic barriers development. These barriers are constituted by elements arranged periodically that are commonly known as "sonic" or "phononic" crystals (see Figure 1). Previous works (for example, see [4–6]) have been developed with the purpose of studying the location of these buried periodic elements relative to the source, dimension, geometric arrangement, as well as the materials to be used to obtain the best efficiency in filtering the most dominant vibration frequencies.

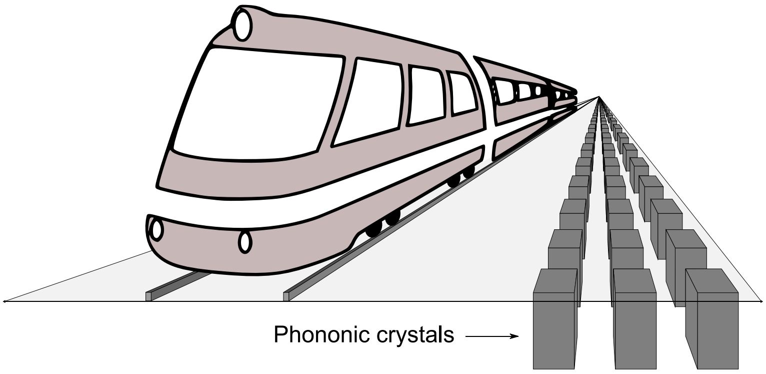

Figure 1 – New mitigation devices (phononic crystals)

Nowadays, the technological and computational advances allow to develop tools capable of simulating wave propagation in an efficient way. This is the case of the inovative time-marching algorithm, developed by Delfim Soares Jr. [7], here implemented on a 3D finite element model.

The purpose of this work is to study the influence of the host medium stratification on the waves propagation induced by heavy transportation vehicles and to predict mitigation strategies adopting the new concept of phononic crystal, using the time-marching algorithm previously mentioned.

WAVE PROPAGATION

The passage of heavy transportation means, in particular the railway traffic, produces mechanical impulses that excite the medium, giving rise to three important types of waves. The compression waves (P) are those with the highest propagation velocity, v_P, defined by equation 1 (E, ν and ρ being the Young's modulus, Poisson's ratio and material density). Those are longitudinal waves causing displacements in the medium, parallel to the direction of the wave. The shear waves (S) are transverse waves causing displacements in the medium, and they are perpendicular to the direction of the propagation. These waves are slower than P waves and their speed, v_S, is defined by equation 2. The surface waves are the slowest. For their low frequency, long duration and large amplitude, these can usually be the most destructive. There are several types of surface waves (such as Rayleigh and Love). For the Rayleigh (R) waves, which propagate along the surface, their velocity, v_R, is approximately that defined in equation 3. These waves cause elliptical orbit displacements in the medium particles and their amplitude decreases rapidly with depth.

$$v_P = \sqrt{\frac{E(1-\nu)}{\rho(1+\nu)(1-2\nu)}} \tag{1}$$

$$v_S = \sqrt{\frac{E}{2\rho(1+\nu)}} \tag{2}$$

$$v_R = \frac{0.87+1.12\nu}{1+\nu}\sqrt{\frac{E}{2\rho(1+\nu)}} \tag{3}$$

NUMERICAL MODEL

In this work it is intended to study the full wavefield generated at the moment of the passage of a train. A loading line is used to simulate the excitation source. The 3D finite element method (FEM) is here used in the time domain, to simulate several scenarios. This method, applied to a dynamic, multidimensional and damped system, can be mathematically defined by the equation 4.

$$\mathbf{F} = \mathbf{F}_\mathrm{I} + \mathbf{F}_\mathrm{D} + \mathbf{F}_\mathrm{S} \tag{4}$$

were $\mathbf{F} = \mathbf{F}(t)$ is the applied load, $\mathbf{F}_\mathrm{I} = \mathbf{M}\ddot{\mathbf{U}}(t)$ is the force of inertia, $\mathbf{F}_\mathrm{D} = \mathbf{C}\dot{\mathbf{U}}(t)$ is the damping force (considering a viscous damping) and $\mathbf{F}_\mathrm{S} = \mathbf{K}\mathbf{U}(t)$ is the elastic force. $\mathbf{M}$, $\mathbf{C}$ and $\mathbf{K}$, are respectively the mass, damping and stiffness matrices. $\ddot{\mathbf{U}}(t)$, $\dot{\mathbf{U}} = \dot{\mathbf{U}}(t)$ and $\mathbf{U} = \mathbf{U}(t)$, are respectively the acceleration, velocity and displacement vectors dependent on time, t. Once $\mathbf{M}$, $\mathbf{C}$ and $\mathbf{K}$ matrices are obtained, the time integration is performed with an innovative algorithm, developed by Soares Jr., presented in [7], where the basic aspects and the main parameters of the new time-marching formulation are described. This paper presents only the time-marching equations used in this new formulation, which are

$$\mathbf{E}\dot{\mathbf{U}}^{n+1} = \mathfrak{I}_\mathbf{F}^{n+\frac{1}{2}} + \mathbf{M}\dot{\mathbf{U}}^n - \frac{1}{2}\Delta t\mathbf{C}\dot{\mathbf{U}}^n - \mathbf{K}\left(\Delta t\mathbf{U}^n + \frac{1}{2}\Delta t^2\dot{\mathbf{U}}^n\right) \tag{5}$$

– the velocity equation – and

$$\mathbf{E}\mathbf{U}^{n+1} = \mathbf{E}\left(\mathbf{U}^n + \frac{1}{2}\Delta t\dot{\mathbf{U}}^n + \frac{1}{2}\Delta t\dot{\mathbf{U}}^{n+1}\right) - \frac{1}{2}\Delta t^2\mathbf{C}\dot{\mathbf{U}}^{n+1} - \mathbf{K}\left[(\beta b_1 b_2)\Delta t^3\dot{\mathbf{U}}^n + \left(\frac{1}{16} + \beta b_1\right)\Delta t^3\dot{\mathbf{U}}^{n+1}\right] \tag{6}$$

– the displacement equation – where $\mathbf{E} = \mathbf{M} + \frac{1}{2}\Delta t\mathbf{C}$ is the effective matrix; n and Δt are the time-step number and time-step length, respectively; $\beta = 1$, $b_1 = 8.567 \times 10^{-3}$ and $b_2 = 8.590 \times 10^{-1}$ are the time integration parameters of the new method; $\mathfrak{I}_\mathbf{F}^{n+1/2} = \beta_1\Delta t\mathbf{F}^n + \beta_2\Delta t\mathbf{F}^{n+1}$, with $\beta_1 = \beta_2 = 1/2$, using trapezoidal quadrature rule or $\beta_1 = 1$ and $\beta_2 = 0$, extending the explicit feature of the technique to the load term (see [7] for more details).

The main features of this model, among others, are: the method is based only on single-step displacement-velocity relations; it requires no system of equations to be dealt with; it is second-order accurate. In other words, this model is very effective, being able to provide accurate analyses considering relatively large time steps (thus, also being very efficient). Moreover, since it has high stability limits, it minimizes the main drawback of explicit procedures, allowing time-steps that are usual in accurate implicit analyses, rendering good results at reduced computational costs [7].

NUMERICAL RESULTS

The present paper follows some previous work by the authors, namelly [4-6]. Here, an important aspect is introduced, namelly the effect of soil stratification in the wave propagation patterns and in the protection provided by periodic deviced. In order to evaluate the efect of such parameters on the vibrations registered at different receivers, the insertion loss was computed for several scenarios and then the results were compared with those obtained for a reference medium.

The mitigation devices correspond to phononic crystals composed by a set of three parallelepipedic inclusions with quadrangular base. Sets of inclusions with four distinct depths, (1.5, 3.0, 5.0 and 7.0) m were studied. For each inclusion length, three levels of stratification were studied, as summarized in the Table 1. The referenced layers in this table are defined in Figure 2 a) and the material properties are defined in Table 2. These fifteen studies were performed using the finite element method that integrates the time-marching algorithm described above.

	Mitigation devices depth [m]														
Host medium	(No mitigation devices)			1.5			3.0			5.0			7.0		
Layer 1	RHM	RHM	RHM	RHM	RHM	RHM	RHM	RHM	RHM	RHM	RHM	RHM	RHM	RHM	RHM
Layer 2	RHM	SHM	SHM	RHM	SHM	SHM	RHM	SHM	SHM	RHM	SHM	SHM	RHM	SHM	SHM
Layer 3	RHM	SHM	R	RHM	SHM	R	RHM	SHM	R	RHM	SHM	R	RHM	SHM	R

RHM – Reference host medium; SHM – Stiffer host medium; R – Rock

Table 1 – Summary of studies carried out

Materials	**Material properties**		
	Density [kg/m³]	Poisson's ratio	Young's modulus [Pa]
Reference host medium	2000	0.35	50×10^6
Stiffer host medium	2000	0.35	200×10^6
Rock	2312	0.23	32×10^9
Mitigating devices	2700	0.20	27×10^9

Table 2 – Material properties

Since the propagation domain is infinite only a 1.2 m slice of the model is considered, which is assumed to be repeated infinitelly along the y direction. Figure 2 a) shows this slice which contains the medium layers, the inclusion set, the loading line and the receivers zone. Adequate boundary conditions were used to simulate the infinite character of the problem. In this work, an absorbing layer 6 m wide was used, based on progressively increasing the material damping towards the outer limits of the model; this layer is responsible for absorbing all the energy that enters it, avoiding unwanted reflections in the system under study. The system is excited by a Ricker pulse generated by a source located 10 m right of the system origin. The phononic crystal has its first element placed at a distance of 10 m to the right of the excitation point. This mitigation device consists of a periodic set of tree inclusions spaced 1.2 m from their centres. Finally, a set of receivers was placed on the surface, in the total width of the slice, 15 m from the source.

Numerical simulations were performed using a 3D FEM in the time domain, formulated using 2 162 160 regular linear tetrahedral elements, whose smallest edges are 0.10 m and the bigger edges are 0.17 m – see Figure 2 b). This mesh was obtained from the Gmsh program (version 2.16.0). The time marching algorithm described above was recently developed by Soares Jr. [7] and is adopted to render the numerical process more efficient. A damping factor equal to 1% and a propagating Ricker pulse with a central frequency of 60 Hz were considered.

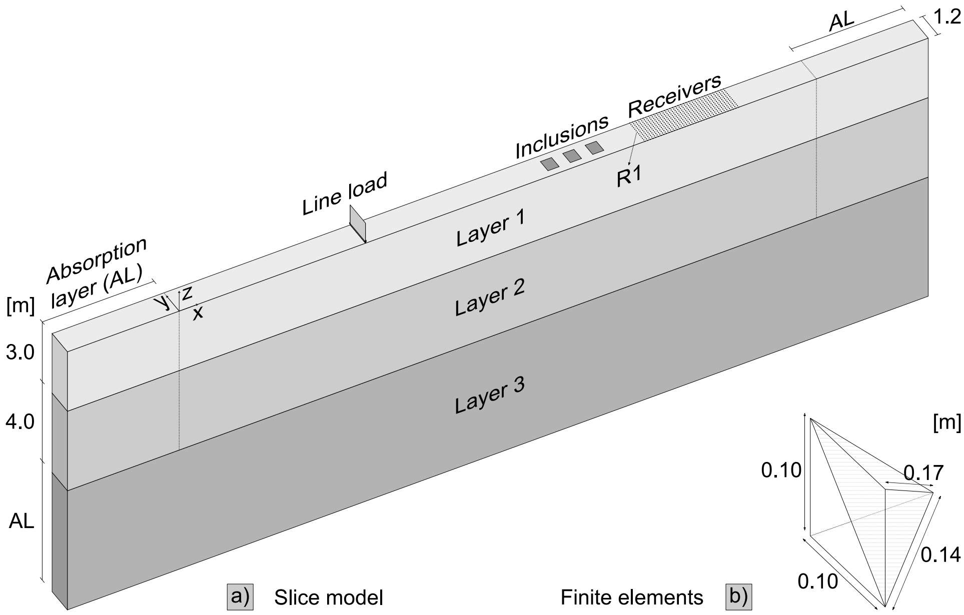

Figure 2 – a) Schematic representation of the slice model used for the wave propagation analysis and b) tetrahedral finite element example

Figure 3 a) shows the vertical amplitudes over time, registered in a receiver, R1 (see Figure 2), placed at the surface of the medium, 15 m from the source, in the alignment of the centre of inclusions. These results are obtained by taking into account three distinct situations: one in which all layers consist of a reference soil (RHM); another in which the Layer 1 is constituted by a reference host medium and the other layers by a stiffer soil (RHM + SHM); and finally, the situation in which the Layer 1 is constituted by a reference host medium, Layer 2 consists of a stiffer soil and the Layer 3 is a stiff rock (RHM + SHM + R) whose material characteristics are defined in Table 2.

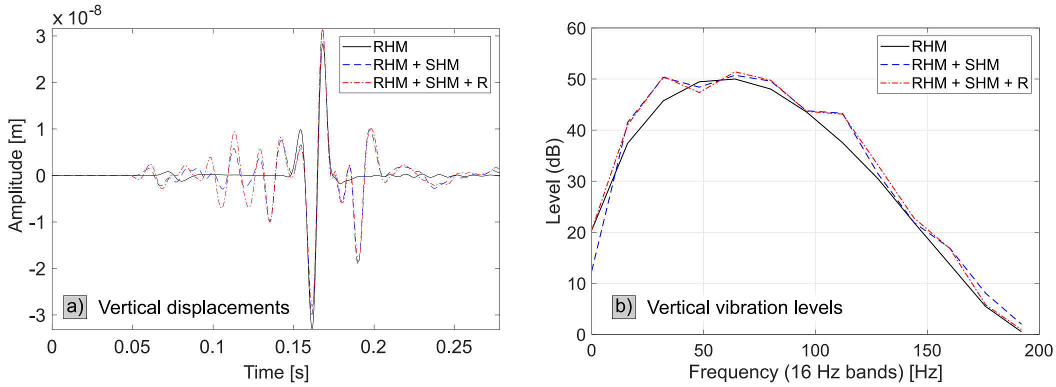

Figure 3 – a) vertical amplitudes over time and b) vertical vibration levels

Figure 3 b) shows the average vibration levels detected on surface receivers 15 m from the source, resulting from vertical displacements, considering the studies carried out. These levels are computed in the frequency domain, after application of a Fourier-transform to the time signals computed using the TD-FEM algorithm. To better observe the global behaviour, the response is grouped in frequency bands 16 Hz wide. From this figure, with respect to the homogeneous medium, it can be seem that stratified medium, considering the stiffer lower layers, generally leads to a higher surface vibration levels at all frequencies.

Figure 4 shows snapshots of the wave field resulting from vertical displacements in the studies carried out: a) only the reference host medium, b) a 3 m reference host medium layer and a stiffer soil below, and finally c) the 3 m reference soil layer, followed by a 4 m stiffer soil layer, followed by a rocky layer. It is evident that, as time progresses, the interference of the progressively stiffer lower layers lead to a more complex wave pattern in the more layered media. Snapshots also reveal that the energy tends to be trapped in the upper layer resulting from the lower layers reflexion. It can also be seen that no spurious reflections from the artificial absorption layer seem to occur.

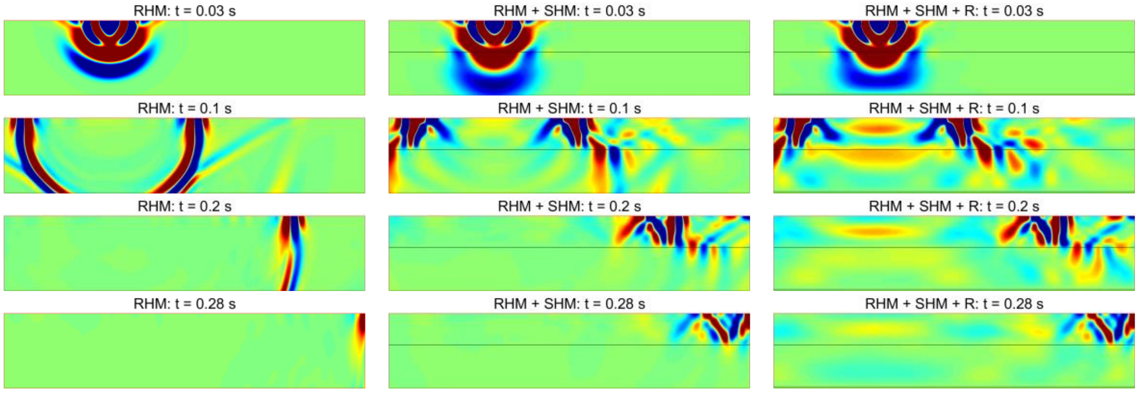

Figure 4 – Propagation over time (vertical displacements) in a) reference medium, b) (reference + stiffer) medium and c) (reference + stiffer) medium + rock

Considering now a set of three inclusions 5 m depth, Figure 5 a) shows the amplitude over time, registered in a receiver, R1, positioned as mentioned in the Figure 3 a) description. It is evident the signal values are smaller than when no mitigation system is present.

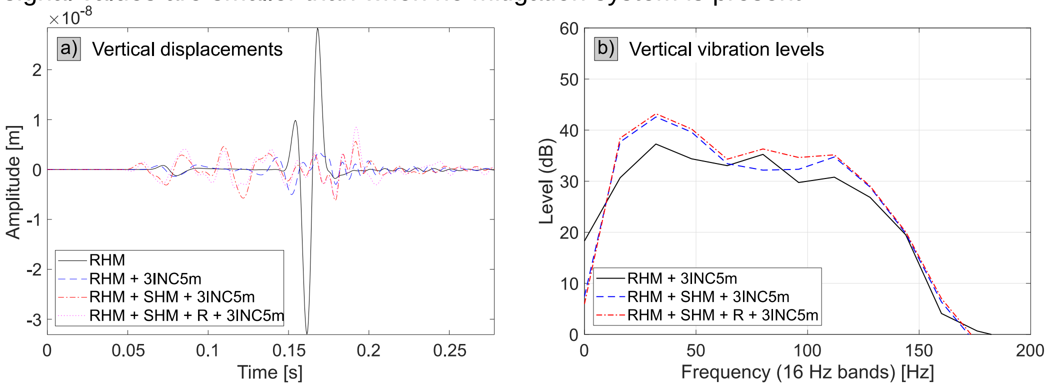

Figure 5 – a) vertical amplitudes over time and b) vertical vibration levels with inclusions

Figure 5 b) shows the average vibration levels registered on surface receivers 15 m from the source, resulting vertical displacements, now considering the 5 m depth inclusions. As previously, these levels are computed in the frequency domain, after application of a Fourier-transform to the time signals computed using the TD-FEM algorithm. The response is grouped in frequency bands 16 Hz wide. From this figure, it can be seem that the presence of the phononic crystals leads to a lower surface vibration levels at all frequencies than those presented previously in Figure 3b.

Figure 6 shows snapshots of the wave field resulting from vertical displacements in the various stratified media considered. It is evident the barrier effect originated by the buried phononic crystals.

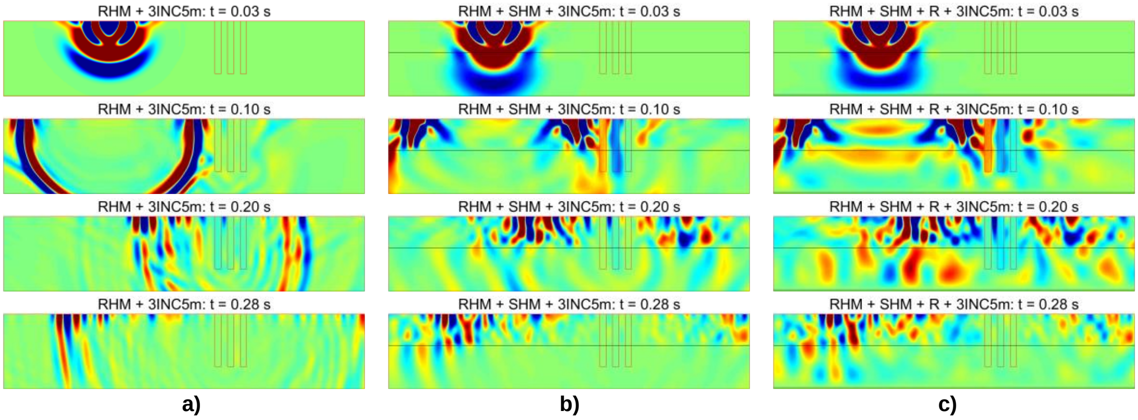

Figure 6 – Propagation over time (vertical displacements) with 5 m depth inclusions in a) reference medium, b) (reference + stiffer) medium and c) (reference + stiffer) medium + rock

To evaluate the effect of the presence of phononic crystals in the vibrations registered in the previously mentioned receivers, the reduction is computed in terms of insertion loss, IL, that is defined as the difference between the vibration levels obtained in the presence of mitigation devices ($L1$) and the displacement vibration levels obtained without those devices ($L0$). This is given in dB by the following Equation 7:

$$IL = L0 - L1 = 20\log|u_0| - 20\log|u_1| \qquad (7)$$

where u_i are the vertical displacements amplitude. According to Equation 7, positive values correspond to a reduction of the displacement vibration levels in the presence of mitigation devices and negative values of the insertion loss stand for losing protective solutions efficiency. In Figure 7, it is seen that in all stratified media studied, there is a reduction of vibration. For all cases, a good mitigation performance is seen approximatelly between 40 Hz and 100 Hz. One should note that considering typical Bragg frequencies for the P and S waves, frequencies of 40 Hz and 83 Hz are obtained, which indicate that the peak attenuation is related with interference effects occuring between scatterers. One should also note that when the inclusions have a depth of 1.5 m much lower attenuations are registered at lower frequencies, indicating that this depth is insufficient to completelly interfere with part of the generated waves.

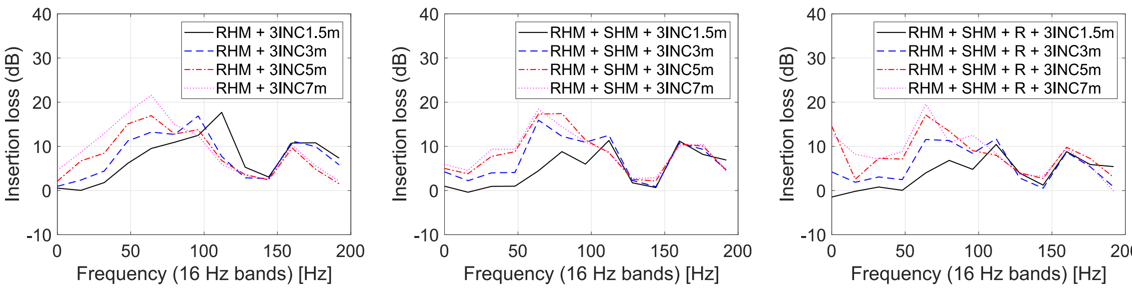

Figure 7 – Insertion loss of mitigating devices in different stratified media

CONCLUSIONS

This work presents a study on the effect of buried phononic crystals in the propagation of vibrations on stratified media. A TD-FEM algorithm is used for this purpose, making use of a recently proposed and efficient time marching scheme. Several simulations were performed in order to better understand the attenuation patterns provided by different configurations. The results are quite promising and reveal the existence of a specific frequency band for which higher vibration attenuation seems to occur. This indicates that using buried phononic crystals can constitute an interesting solution for mitigation of vibrations at specific frequency bands, while still ensuring interesting attenuations outside these specific bands.

ACKNOWLEDGEMENTS

The authors acknowledge the financial support of FCT – Foundation for Science and Technology and COMPETE, through research project PTDC/ECM-COM/1364/2014 (METASHIELD). This work is also financed by FEDER funds through the Competitivity Factors Operational Programme - COMPETE and by national funds through FCT – Foundation for Science and Technology within the scope of the projects POCI-01-0145-FEDER-007633 (ISISE) and POCI-01-0145-FEDER-007457 (CONSTRUCT). The authors acknowledge the financial support of Regional Operational Programme CENTRO2020 within the scope of the project CENTRO-01-0145-FEDER-000006 (SUSpENsE).

REFERENCES

[1] M.G. Smith, I. Croy, M. Ögren, K.P. Waye, On the Influence of Freight Trains on Humans: A Laboratory Investigation of the Impact of Nocturnal Low Frequency Vibration and Noise on Sleep and Heart Rate, PLoS One. 8(2): e558 (2013). doi:10.1371/journal.pone.0055829.

[2] I. Croy, M.G. Smith, K.P. Waye, Effects of train noise and vibration on human heart rate during sleep: an experimental study, BMJ Open. (2013). doi:10.1136/bmjopen-2013-002655.

[3] Y.B. Yang, H.H. Hung, Wave Propagation for Train-Induced Vibrations. A Finite/Infinite Element Approach, World Scientific Publishing Co. Pte. Ltd., Singapore, 2009.

[4] C. Albino, L. Godinho, D. Dias-da-Costa, P. Amado-Mendes, The MFS as a tool for the numerical analysis of vibration protection devices, in: 22nd Int. Congr. Acoust. (ICA 2016), Buenos Aires, 2016.

[5] L. Godinho, C. Albino, P. Alves-Costa, P. Amado-Mendes, A.C. Pinto, D. Soares Jr., Numerical study of a buried periodic device for vibration protection, in: Euronoise 2018, Crete, Greece, 2018: pp. 1329–1335.

[6] L. Godinho, P. Amado-Mendes, P. Alves-Costa, C. Albino, MFS Analysis Of The Vibration Filtering Effect Of Periodic Structures In Elastic Media, Int. J. Comput. Methods Exp. Meas. 6 (2018) 1108–1119. doi:10.2495/CMEM-V6-N6-1108-1119.

[7] D. Soares Jr., A novel family of explicit time marching techniques for structural dynamics and wave propagation models, Comput. Methods Appl. Mech. Eng. 311 (2016) 838–855. doi:http://dx.doi.org/10.1016/j.cma.2016.09.021.